



Magnetic and transport properties of Ni_2MnGa – BaTiO_3 metal–insulator particulate composite with percolation threshold

C.J. Won, R.C. Kambale, N. Hur*

Department of Physics, Inha University, Incheon 402-751, Republic of Korea

ARTICLE INFO

Article history:

Received 22 November 2010

Received in revised form 29 March 2011

Accepted 2 April 2011

Available online 8 April 2011

Keywords:

Composite materials

Solid state reactions

Electrical transport

Magnetoresistance

X-ray diffraction

Magnetic measurements

ABSTRACT

Here we report the magnetic and transport properties of the metal/insulator (f_{NMG}) $\text{Ni}_2\text{MnGa}/(1 - f_{\text{NMG}})\text{BaTiO}_3$ composites. The X-ray diffraction study confirms the formation of both the phases in composite. The microstructure reveals that the conducting Ni_2MnGa particles are well dispersed in an insulating BaTiO_3 matrix. Temperature dependent magnetization shows two transitions one above 300 K and other below 150 K. The temperature dependence resistivity near the percolation threshold $f_{\text{NMG}} = 0.4$ had drastic changes which is higher than the $f_{\text{NMG}} = 0.5$. Also the negative magnetoresistance effect was observed for the studied materials. We suggest that magnetic and transport properties at the percolation threshold can be adjusted by the strain from the surrounding insulator particle.

© 2011 Elsevier B.V. All rights reserved.

1. Introduction

Although application of colossal magnetoresistance (CMR) has not been realized yet, CMR is expected to have great opportunities for the development of new technologies such as magnetic sensor, spintronic devices [1–4]. Especially, in phase separated perovskite manganites which simultaneously exhibit charge ordered antiferromagnetic insulating state and ferromagnetic metallic state, CMR effects with several orders of magnitude were observed when the charged ordered antiferromagnetic insulating state was converted to the ferromagnetic metallic state by external magnetic fields [5–10]. In phase separated CMR manganites, a percolating network of interconnected ferromagnetic metallic filaments induces dramatic resistivity changes through the variation of magnetic field and temperature [11,12].

In other words, the percolative magnetoresistance (MR) effect in phase separated CMR manganites occurs due to the increase of volume of metallic phase through the transition from charge ordered antiferromagnetic insulating phase to ferromagnetic metallic phase by applied magnetic field [13]. Such percolative MR effect emerges not only in phase-separated single phase materials but also in metal/insulator composites [14–19]. In ferromagnet/insulator composite, for instance, the low field MR was observed due to spin polarized tunneling [14–19]. Recently, CMR about $10^5\%$ was

observed in the composites compounded near the percolation threshold [20]. For such case it was reported that the Curie temperature (T_c) of ferromagnetic metallic phase was modified due to strain from surrounding second phase component. Previous reports on the electrical transport in metal/insulator (M/I) composites showed that a high MR has been detected around percolation threshold and MR was affected by the strain between metallic and surrounding insulating phase [20].

In this work, we report the magnetic and transport properties of metal (Ni–Mn–Ga)/insulator (BaTiO_3) composites prepared by solid state reaction (ceramic method). NMG is the Heusler alloy with $L2_1$ structure, which is the body-centered cubic with a face-centered superlattice, and BTO has perovskite structure with general formula ABO_3 , which consists of a framework of Ti octahedra [21,22]. Ni–Mn–Ga (NMG) is selected because it is a ferromagnetic shape memory alloy (SMA) having large magnetic field induced strain through structure transition, and is used as actuators, sensors and in energy-harvesting devices [23–30]. While, BaTiO_3 (BTO) is chosen as an insulator phase for M/I composite due to its excellent dielectric and ferroelectric properties [22,31,32]. This kind of material which consists of magnetostrictive and ferroelectric material has been reported to have potential application in the ME sensors. For example, although the piezoelectric lead based materials or BTO and piezomagnetic Terfenol-D or cobalt ferrite have no magnetoelectric effect individually, their composites have ME effects as a result of the elastic interaction [33–36]. Here, we report the influence of volume fraction of the NMG on the electrical transport of particulate composites near to the percolation

* Corresponding author. Tel.: +82 32 860 7651; fax: +82 32 872 7562.

E-mail address: nhur@inha.ac.kr (N. Hur).

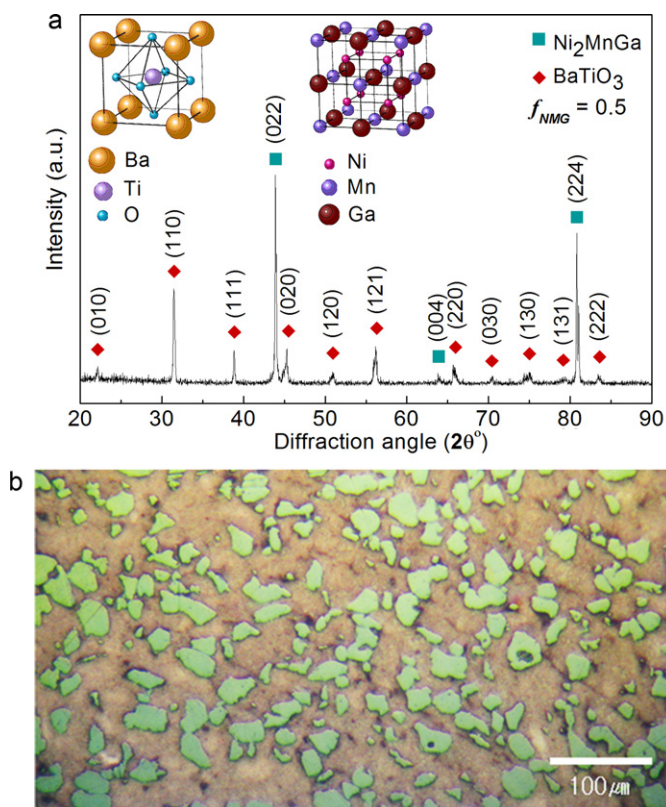


Fig. 1. (a) Typical room temperature XRD pattern of $\text{Ni}_2\text{MnGa}/\text{BaTiO}_3$ with $f_{\text{NMG}} = 0.5$ and (b) Polarized cross-section microscope image of $\text{Ni}_2\text{MnGa}/\text{BaTiO}_3$ with $f_{\text{NMG}} = 0.5$. In the inset, (left) the crystal structure of BaTiO_3 and (right) that of Ni_2MnGa were displayed.

threshold using a series of NMG metal/BTO insulator composites (volume fraction $f_{\text{NMG}} = 0, 0.4, 0.5$, and 1).

2. Experimental details

The NMG/BTO composites were prepared by using conventional solid state reaction. The Ni–Mn–Ga samples were prepared in an evacuated quartz tube and the raw materials like Ni powder (99.996%), Mn powder (99.95%), and Ga ingot (99.9999%) were used for the preparation of NMG with 2:1:1 molar ratio of Ni:Mn:Ga respectively. The raw materials of NMG were taken in their appropriate molar ratio was mixed together and grounded in an agate mortar for 1 h. The grounded sample of NMG was sintered at 1000 °C in an evacuated quartz tube for 48 h. After sintering, the whole mixture was reground for 2 h in order to achieve better homogeneity and again re-sintered at 1000 °C in an evacuated quartz tube for 48 h to get the final product. Similarly, the BTO powder was also prepared by the solid state reaction with the raw materials BaCO_3 (99.997%) and TiO_2 (99.99%, Alfa Aesar). The raw materials of BTO were mixed together in the molar ratio of 1:1 of BaCO_3 and TiO_2 respectively in an agate mortar for 1 h and sintered at 1350 °C in a programmable furnace for 48 h with intermediate grinding.

The prepared powder of NMG was mixed with BTO in a volume ratio of $f_{\text{NMG}}:(1 - f_{\text{NMG}})$, with $f_{\text{NMG}} = 0, 0.35, 0.4, 0.5$, and 1 where f_{NMG} is the volume fraction of NMG. The mixture was reground in an agate mortar for 1 h and finally sintered at 1000 °C in an evacuated quartz tube for 48 h. The X-ray diffraction (XRD diffractometer, Rigaku DMAX 2500 with Cu K α radiation) was used to confirm the presence of NMG and BTO in the composite. Microstructure was observed by using polarized optical microscope. The temperature dependence of magnetization were studied in the temperature range of 400–5 K in the magnetic field of 100 Oe by using a vibrating sample magnetometer (VSM) connected to the quantum design physical property measurement system (PPMS). The temperature and magnetic field (1 T) dependence of the electrical resistivity was measured by using 4 probe method.

3. Results and discussion

3.1. Structural analysis

Fig. 1a shows the typical X-ray diffraction (XRD) pattern for NMG–BTO composite with $f_{\text{NMG}} = 0.5$. The XRD pattern shows well

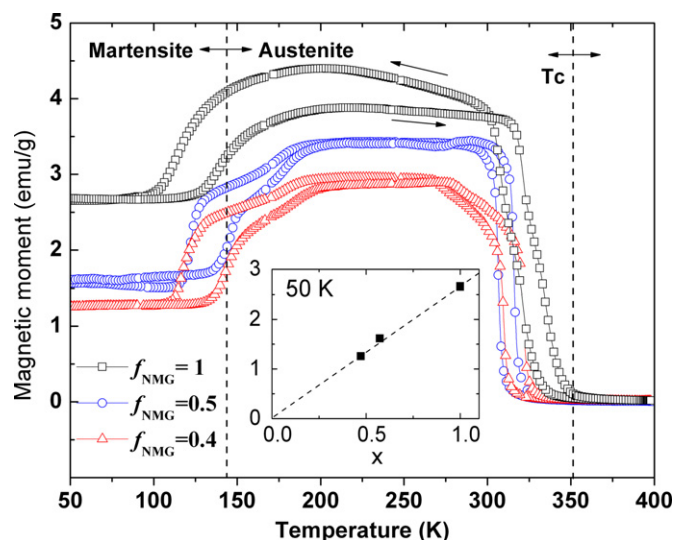


Fig. 2. Temperature dependence of magnetization for $\text{Ni}_2\text{MnGa}-\text{BaTiO}_3$ composites with $f_{\text{NMG}} = 0.4, 0.5$, and 1. In the inset, the magnetizations of the composites with NMG mass contents x was displayed.

polycrystalline nature of the composite and the results obtained by XRD are in good agreements with the standard JCPDS data (Card No. 50-1518 and 05-0626). The XRD results clearly reveal the two sets of diffraction patterns corresponding to NMG and BTO phases without any impurity patterns confirming that there is no chemical reaction which has occurred between BTO and NMG phases.

Fig. 1b shows the polarized optical microscope image of NMG–BTO composite with $f_{\text{NMG}} = 0.5$. It is seen that the conducting NMG particles (green) gets covered by an insulating BTO (gray) matrix. Also, it is observed that the BTO particles get dispersed around the NMG particles and they are of irregular shape and size. The grain size of the NMG alloy is found to be of the order of 1–10 μm . The NMG grains are close to each other in microscope image, so NMG grains can make the filamentary paths in NMG–BTO composite.

Fig. 2 shows the temperature dependence of magnetization (thermal hysteresis) with heating and cooling curves of NMG–BTO composites with $f_{\text{NMG}} = 0.4, 0.5$, and 1. There are two sudden changes observed at above 300 K and below 150 K; the former is attributed to the ferromagnetic transition, and latter is attributed to the Martensite to Austenite structure transition which have thermal hysteresis by first order transition [37]. Compared with the temperature dependence of magnetization of the NMG–BTO, $f_{\text{NMG}} = 1$, the Curie temperature as well as the Martensite to Austenite structural transition temperature for the case of $f_{\text{NMG}} = 0.4$ and $f_{\text{NMG}} = 0.5$ is different that of from $f_{\text{NMG}} = 1$. Such type of difference may be observed due to slight chemical reaction and strain effect in composite due to sintering effect [38]. Here, we observed that the magnetization of composites increases linearly with increasing molar content of NMG phase, x (inset of Fig. 2). The molar contents for the case of $f_{\text{NMG}} = 0.4$ is $x_{\text{NMG}} = 0.471$, and the case of $f_{\text{NMG}} = 0.5$ is $x_{\text{NMG}} = 0.572$.

If NMG bulk forms the filamentary path in BTO matrix with increasing volume fraction of f_{NMG} , the resistance of the samples is expected to change dramatically. Fig. 3a shows the temperature dependence of electrical resistivity of NMG–BTO composites with $f_{\text{NMG}} = 0.35, 0.4, 0.5$, and $f_{\text{NMG}} = 1$. It is observed that as f_{NMG} increases the resistivity of the composite decreases due to low resistance of NMG ($\sim 10^{-3} \Omega \text{cm}$) phase than that of the BTO phase. The samples $f_{\text{NMG}} = 0.35$ and 0.4 shows an insulator-like behavior, whereas the sample of $f_{\text{NMG}} = 0.5$ shows a metal-like behavior. This kind of observation, clearly depicts that the difference of resistivity with volume fraction in NMG establish the percolation thresh-

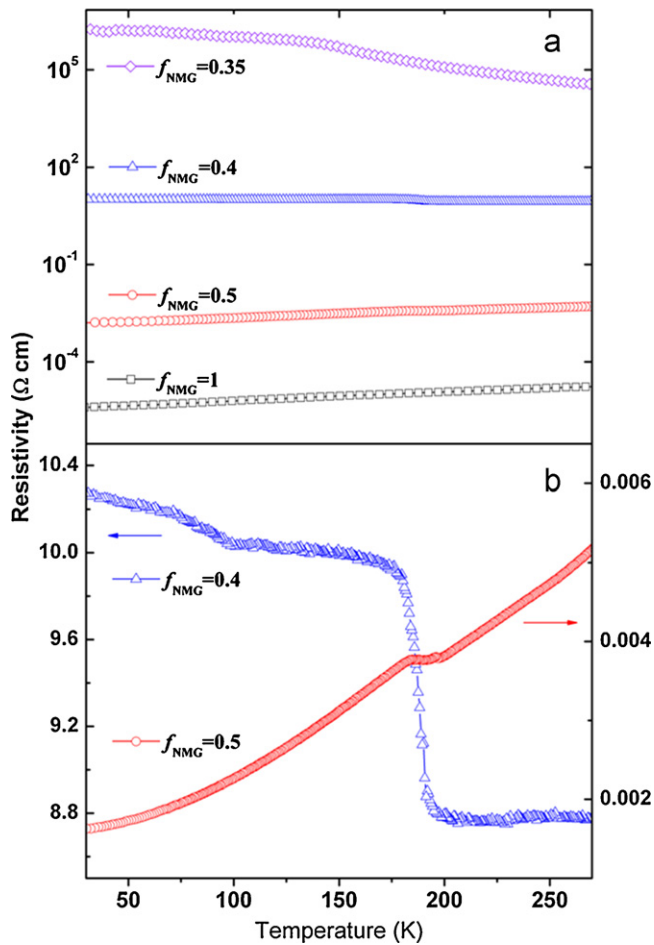


Fig. 3. The temperature dependence of resistivity of $\text{Ni}_2\text{MnGa-BaTiO}_3$ with $f_{\text{NMG}} = 0.35, 0.4, 0.5$, and $f_{\text{NMG}} = 1$.

old in this metal/insulator composites and which is in between $f_{\text{NMG}} = 0.4$ and 0.5 . Theoretically, in metal-insulator composites, the critical volume fraction of percolation threshold was calculated by Scher and Zallen, and it was 0.16 ± 0.02 [39]. In present study, the observed percolation threshold is higher than reported by Scher and Zallen, and the resistivity of $f_{\text{NMG}} = 0.35$ at room temperature is still very high and has insulator-like behavior.

Most of the percolation thresholds reported in previous papers were different from theoretical percolation threshold: 0.12–0.19 for LCMO/insulator, 0.2–0.55 for LSMO/insulator, 0.07–0.28 for carbon conductor/polymer [40–42]. The percolation threshold, based on the periodic structure by Scher and Zallen [39], is different from the experimental percolation threshold which could be affected by porosity, poor boundary, and grain size. In view of Fig. 1b, fine BTO grains percolate through the larger NMG grains and interrupt the conducting path of NMG. The NMG particles of percolation path must connect with other NMG particles in between the BTO matrix. In this case, the percolation threshold can become much higher than the theoretical one as predicted by de Bondt et al. [43]. In their model, some granular systems composed of metal and insulator with a large difference in their grain size have critical metallic volume fractions $x_c \sim 40\%$ [43]. Thus we infer that higher critical f_{NMG} in our experiment is mainly due to the large difference grain size between NMG and BTO, and also possibly due to the porosity of BTO, which effectively increase the volume fraction of insulator.

In Fig. 3b, the resistivity of composites with $f_{\text{NMG}} = 0.4$ near 190 K are sharply increased 13% compared with at room temperature, and that with $f_{\text{NMG}} = 0.5$ has anomaly or increase at same temperature

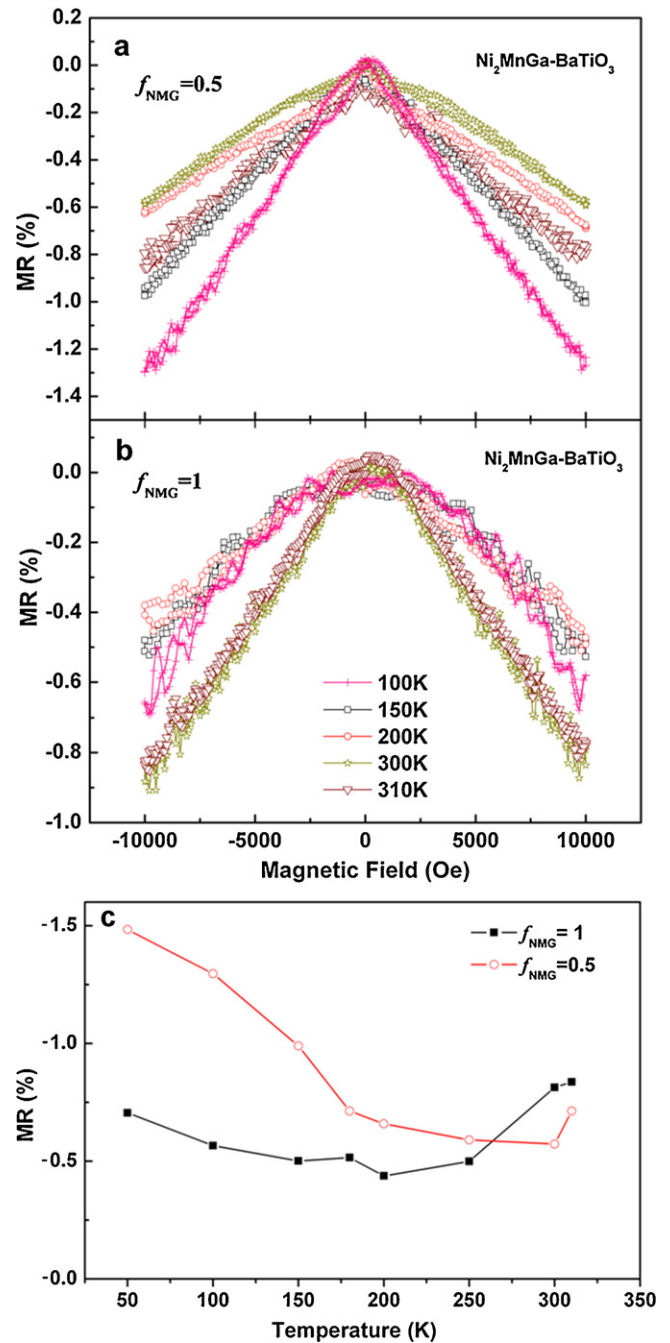


Fig. 4. (a) The magnetoresistance coefficient for $\text{Ni}_2\text{MnGa-BaTiO}_3$ composites with $f_{\text{NMG}} = 0.5$ and (b) 1 at various temperatures. (c) Variation of MR coefficient as a function of temperature for $\text{Ni}_2\text{MnGa-BaTiO}_3$ composites with $f_{\text{NMG}} = 0.5$ and 1.

(as not shown). As shown in Fig. 2, the martensite transition temperature is lower than 190 K, whereas the temperature of structure transition of BTO is close to 190 K. The composite with $f_{\text{NMG}} = 0.5$, higher than percolation threshold, has less anomaly than the case of $f_{\text{NMG}} = 0.4$ at the same temperature. Therefore, we suggest that the drastic anomaly of resistivity is owing to the filamentary path with NMG particles affected by strain which is caused by the structure transition of BTO near the percolation threshold.

Fig. 4a and b show the variation MR coefficient for NMG-BTO composites with $f_{\text{NMG}} = 0.5$ and 1 as a function of applied magnetic field at various temperatures, respectively. The MR coefficient for $f_{\text{NMG}} = 0.5$ is found to be more than the MR coefficient of $f_{\text{NMG}} = 1$ in most of the temperature range except near the room temperature.

Also, it is observed that for $f_{\text{NMG}} = 0.5$, the MR coefficient is -0.6% at 300 K which increases up to -1.5% at 50 K with decreasing the temperature (Fig. 4c). This behavior may be attributed to the tunneling MR effect through NMG grain boundaries in BTO matrix. However, at 310 K the MR coefficient was found to be increased for $f_{\text{NMG}} = 0.5$ and 1 by a small value as compared to MR of 300 K, which appears to be due to the increased MR effect near the ferromagnetic transition above 300 K (Fig. 2). Smaller MR values of $f_{\text{NMG}} = 0.5$ compared to MR of $f_{\text{NMG}} = 1$ near the room temperature may be due to the ferromagnetic transition as well as the influence of surrounding BTO phase which causes the strain on NMG domain.

4. Conclusion

The metal/insulator composites of NMG-BTO were successfully prepared by solid state reaction. XRD results confirm that no chemical reaction occurred between NMG and BTO particles. Temperature dependent magnetization shows the ferromagnetic transition at above 300 K and also shows the Martensite to Austenite structure transition below 150 K. The magnetic and electrical transport of metal/insulator (NMG/BTO) composites shows the resistivity change associated to filamentary conducting path at percolation threshold. In the metal/insulator composite, the strains by surrounding second phase affect the electrical transport of composites. The negative magnetoresistance effect was observed for the studied compositions. The MR coefficient is found to decrease with increase of temperature below room temperature.

Acknowledgments

This work was supported by Korea Research Foundation through KRF-2008-331-C00093.

References

- [1] C. Felser, G.H. Fecher, B. Balke, Spintronics: a challenge for materials science and solid-state chemistry, *Angew. Chem. Int. Ed.* 46 (2007) 668–699.
- [2] S. Jin, M. McCormack, T.H. Tiefel, R. Ramesh, Colossal magnetoresistance in La–Ca–Mn–O ferromagnetic thin films, *J. Appl. Phys.* 76 (1994) 6929–6933.
- [3] W. Prellier, B. Ph Lecoer, Mercey, Colossal-magnetoresistive manganite thin films, *J. Phys. Condens. Matter* 13 (2001) R915–R944.
- [4] V.A. Vas'ko, V.A. Larkin, P.A. Kraus, K.R. Nikolaev, D.E. Grupp, C.A. Nordman, A.M. Goldman, Critical current suppression in a superconductor by injection of spin-polarized carriers from a ferromagnet, *Phys. Rev. Lett.* 78 (1997) 1134–1137.
- [5] S. Jin, T.H. Tiefel, M. McCormack, R.A. Fastnacht, R. Ramesh, L.H. Chen, Thousandfold change in resistivity in magnetoresistive La–Ca–Mn–O films, *Science* 264 (1994) 413–415.
- [6] S. Jin, H.M. O'Bryan, T.H. Tiefel, M. McCormack, W.W. Rhodes, Large magnetoresistance in polycrystalline La–Y–Ca–Mn–O, *Appl. Phys. Lett.* 66 (1995) 382–384.
- [7] J.H. van Santen, G.H. Jonker, Electrical conductivity of ferromagnetic compounds of manganese with perovskite structure, *Physica* 17 (1950) 599–600.
- [8] A. Asamitsu, Y. Morimoto, Y. Tomioka, T. Arima, Y. Tokura, A structural phase transition induced by an external magnetic field, *Nature* 373 (1995) 407–409.
- [9] R. von Helmolt, J. Wecker, B. Holzapfel, L. Schultz, K. Samwer, Giant negative magnetoresistance in perovskite $\text{La}_{2/3}\text{Ba}_{1/3}\text{MnO}_x$ ferromagnetic films, *Phys. Rev. Lett.* 71 (1993) 2331–2333.
- [10] M. Uehara, S. Mori, C.H. Chen, S.-W. Cheong, Percolative phase separation underlies colossal magnetoresistance in mixed-valent manganites, *Nature* 399 (1999) 560–563.
- [11] K. Lai, M. Nakamura, W. Kundhikanjana, M. Kawasaki, Y. Tokura, M.A. Kelly, Z.-X. Shen, Mesoscopic percolating resistance network in a strained manganite thin film, *Science* 329 (2010) 190–193.
- [12] L. Zhang, C. Israel, A. Biswas, R.L. Greene, A. de Lozanne, Direct observation of percolation in a manganite thin film, *Science* 298 (2002) 805–807.
- [13] W. Wu, C. Israel, N. Hur, S. Park, S.-W. A. Cheong, de Lozanne, Magnetic imaging of a supercooling glass transition in a weakly disordered ferromagnet, *Nat. Mater.* 5 (2006) 881–886.
- [14] J.H. Miao, L. Yuan, Y.Q. Wang, J.L. Shang, G.Q. Yu, G.M. Ren, X. Xiao, S.L. Yuan, Electrical transport and magnetoresistance in $\text{La}_{2/3}\text{Ca}_{1/3}\text{MnO}_3/\text{CuO}$ composites, *Mater. Lett.* 20 (2006) 2214–2216.
- [15] L.E. Hueso, J. Rivas, F. Rivadulla, M.A. López-Quintela, Magnetoresistance in manganite–alumina nanocrystalline composites, *J. Appl. Phys.* 89 (2001) 1746–1750.
- [16] X.S. Yang, X.S. Yang, Y. Yang, W. He, C.H. Cheng, Y. Zhao, Low-field magnetoresistance in $\text{La}_{0.7}\text{Sr}_{0.3}\text{MnO}_3/\text{Ta}_2\text{O}_5$ composites, *J. Phys. D: Appl. Phys.* 41 (2008) 115009.
- [17] D.K. Petrov, L. Krusin-Elbaum, J.Z. Sun, C. Feild, P.R. Duncombe, Enhanced magnetoresistance in sintered granular manganite/insulator systems, *Appl. Phys. Lett.* 75 (1999) 995–997.
- [18] A. Milner, A. Gerber, B. Groisman, M. Karpovsky, A. Gladkikh, Spin-dependent electronic transport in granular ferromagnets, *Phys. Rev. Lett.* 76 (1996) 475–478.
- [19] S. Gupta, R. Ranjit, C. Mitra, P. Raychaudhuri, R. Pinto, Enhanced room-temperature magnetoresistance in $\text{La}_{0.7}\text{Sr}_{0.3}\text{MnO}_3$ -glass composites, *Appl. Phys. Lett.* 78 (2001) 382–384.
- [20] V. Moshynaya, B. Damaschke, O. Shapoval, A. Belenchuk, J. Faupel, O.I. Lebedev, J. Verbeeck, G. van Tendeloo, M. Mücksch, V. Tsurkan, R. Tidecks, K. Samwer, Structural phase transition at the percolation threshold in epitaxial $(\text{La}_{0.7}\text{Ca}_{0.3}\text{MnO}_3)_{1-x}(\text{MgO})_x$ nanocomposite films, *Nat. Mater.* 2 (2003) 247–252.
- [21] A.J. Bradley, J.W. Rogers, The crystal structure of the heusler alloys, *Proc. R. Soc. A144* (1934) 340–359.
- [22] A. von Hippel, Ferroelectricity, domain structure, and phase transitions of barium titanate, *Rev. Mod. Phys.* 22 (1950) 221–237.
- [23] K. Ullakko, J.K. Huang, C. Kantner, R.C. O'Handley, V.V. Kokorin, Large magnetic-field-induced strains in Ni_2MnGa single crystals, *Appl. Phys. Lett.* 69 (1996) 1966–1968.
- [24] A. Sozinov, A.A. Likhachev, K. Ullakko, Crystal structures and magnetic anisotropy properties of Ni–Mn–Ga martensitic phases with giant magnetic-field-induced strain, *IEEE Trans. Magn.* 38 (2002) 2814–2816.
- [25] S.J. Murray, M. Marioni, S.M. Allen, R.C. O'Handley, T.A. Lograsso, 6% magnetic-field-induced strain by twin-boundary motion in ferromagnetic Ni–Mn–Ga, *Appl. Phys. Lett.* 77 (2000) 886–888.
- [26] A. Sozinov, A.A. Likhachev, N. Lanska, K. Ullakko, Giant magnetic-field-induced strain in NiMnGa seven-layered martensitic phase, *Appl. Phys. Lett.* 80 (2002) 1746–1748.
- [27] N. Sarawate, M. Dapino, Experimental characterization of the sensor effect in ferromagnetic shape memory Ni–Mn–Ga, *Appl. Phys. Lett.* 88 (2006) 121923.
- [28] J. Tellinen, I. Suorsa, A. Jääskeläinen, I. Aaltio, K. Ullakko, Basic properties of magnetic shape memory actuators, in: 8th international conference ACTUATOR, 2002.
- [29] I. Karaman, B. Basaran, H.E. Karaca, A.I. Karsilayan, Y.I. Chumlyakov, Energy harvesting using martensite variant reorientation mechanism in a NiMnGa magnetic shape memory alloy, *Appl. Phys. Lett.* 90 (2007) 172505.
- [30] M. Chmielus, X.X. Zhang, C. Witherspoon, D.C. Dunand, P. Müllner, Giant magnetic-field-induced strains in polycrystalline Ni–Mn–Ga foams, *Nat. Mater.* 8 (2009) 863–866.
- [31] C. Kittel, Introduction to Solid State Physics, 7th ed., John Wiley & Sons, Inc., United States of America, 1996.
- [32] N.W. Ashcroft, N.D. Mermin, Solid State Physics International Edition, Saunders college publishing, United States of America, 1976.
- [33] H. Zheng, J. Wang, S.E. Lofland, Z. Ma, L. Mohaddes-Ardabili, B. Ogale, F. Bai, D. Viehland, Y. Jia, D.G. Schlom, M. Wuttig, A. Roytburd, R. Ramesh, Multiferroic $\text{BaTiO}_3\text{--CoFe}_2\text{O}_4$ nanostructures, *Science* 303 (2004) 661–663.
- [34] Y. Wang, X. Zhao, J. Jiao, L. Liu, W. Di, H. Luo, S. Wing Or, Electrical resistance load effect on magnetoelectric coupling of magnetostrictive/piezoelectric laminated composite, *J. Alloys Compd.* 500 (2010) 224–226.
- [35] J.-P. Zhou, L.-M. Meng, Z.-H. Xia, P. Liu, G. Liu, Inhomogeneous magnetoelectric coupling in $\text{Pb}(\text{Zr,Ti})\text{O}_3/\text{Terfenol-D}$ laminate composite, *Appl. Phys. Lett.* 92 (2008) 062903.
- [36] J. Ma, Z. Shi, C.-W. Nan, Magnetoelectric properties of composites of single $\text{Pb}(\text{Zr,Ti})\text{O}_3$ rods and Terfenol-D/Epoxy with a single-period of 1-3-type structure, *Adv. Mater.* 19 (2007) 2571–2573.
- [37] S. Banik, A. Chakrabarti, U. Kumar, P.K. Mukhopadhyay, A.M. Awasthi, R. Ranjan, J. Schneider, B.L. Ahuja, S.R. Barman, Phase diagram and electronic structure of $\text{Ni}_{2-x}\text{Mn}_{1-x}\text{Ga}$, *Phys. Rev. B* 74 (2006) 085110.
- [38] S.-Y. Chu, R. Gallagher, M. De Graef, M.E. McHenry, Structural and magnetic phase transitions in Ni–Mn–Ga ferromagnetic shape-memory crystals, *IEEE Trans. Magn.* 37 (2007) 2666–2668.
- [39] H. Scher, R. Zallen, Critical density in percolation processes, *J. Chem. Phys.* 53 (1970) 3759–3761.
- [40] B. Vertruyen, R. Cloots, M. Ausloos, J.-F. Fagnard, Ph. Vanderbemden, Electrical transport and percolation in magnetoresistive manganite/insulating oxide composites: case of $\text{La}_{0.7}\text{Ca}_{0.3}\text{MnO}_3/\text{Mn}_2\text{O}_4$, *Phys. Rev. B* 75 (2007) 165112.
- [41] J. Liang, Q. Yang, Aggregate structure and percolation behavior in polymer/carbon black conductive composites, *J. Appl. Phys.* 102 (2007) 083508.
- [42] D.K. Petrov, L. Krusin-Elbaum, J.Z. Sun, C. Field, P.R. Duncombe, Enhanced magnetoresistance in sintered granular manganite/insulator systems, *Appl. Phys. Lett.* 75 (1999) 995–997.
- [43] S. de Bondt, L. Froyen, A. Deruyttere, Electrical conductivity of composites: a percolation approach, *J. Mater. Sci.* 27 (1992) 1983–1988.